2-D Analytical Model for Computing Eddy-Current Loss in Nonlinear Thick Steel Laminations

Ismet Tuna Gürbüz[1], Paavo Rasilo[2], Floran Martin[1], Osaruyi Osemwinyen[1], and Anouar Belahcen[1]

[1]Department of Electrical Engineering and Automation, Aalto University, 00076 Espoo, Finland
[2]Unit of Electrical Engineering, Tampere University, 33720 Tampere, Finland

In this article, we propose an analytical method to compute the eddy-current loss in nonlinear thick steel laminations (3–12 mm) by considering the return path of the eddy currents. Initially, a 2-D finite-element (FE) model is applied to segregate losses measured from toroidal material samples into hysteresis and eddy-current loss components to use them as reference. Afterward, a 2-D analytical time-domain model is proposed for the eddy currents based on the solution of the 2-D field problem. The time-domain model is then used to derive a simple frequency-domain eddy-current loss formulation for the sinusoidal flux density case with the inclusion of a skin-effect correction factor, which accounts for the nonlinearity of the material. Highly accurate results are obtained from the proposed model compared to FE reference results with a mean relative error of 5.1% in the nonlinear region.

Index Terms— **Eddy currents, eddy-current loss, nonlinearity, skin effect, thick steel laminations.**

I. Introduction

THE attempts in decreasing the manufacturing costs in the construction of large-diameter synchronous machines bring over the use of thick laminations (i.e., 3–12 mm) in the rotor pole shoes. Although this use is efficient in terms of the manufacturing costs, it causes additional challenges in proper modeling of eddy-current loss due to the return path of eddy currents, and prominent skin effect across the lamination cross section. In order to predict the eddy-current loss for thick laminations properly, these challenges should be accounted for in the modeling stage.

In the literature, several studies were conducted to compute the eddy-current loss numerically from the magnetic field solution. In [1]–[3], the eddy currents were modeled in 1-D along the lamination thickness by including the skin effect and then coupled with the 2-D field solution. In [4] and [5], the return path of the eddy currents were included and the eddy currents were modeled in 2-D. In [6], a 2-D axisymmetric finite-element (FE) model along the lamination cross section with a hysteretic constitutive law was presented, and this model was developed further in [7] by including the effect of cutting for 12 mm thick laminations. These studies showed that 2-D FE modeling of the eddy currents provides highly accurate results and enables proper segregation of the losses. However, coupling of these 2-D models along the lamination with the 2-D field solution of an electrical machine can be challenging and computationally inefficient.

To compute the eddy-current loss faster and in a simpler way, analytical formulas were proposed and used in the post-processing of the numerical field solution. Among these formulas, time-domain formulas [8], [9] were derived based on the Bertotti's *low-frequency approach* [10], and modified to include the skin effect in the calculation. Similarly, the frequency-domain formulas for the sinusoidal excitation are also majorly based on Bertotti's formula [10]. Usually, these formulas are used for thin laminations (e.g., 0.5 mm) considering that lamination width w is so much larger than lamination thickness d, i.e., $w \gg d$. These models do not provide good accuracy for the characterization of the thick laminations, when w and d are comparable, and skin effect is dominant even at low frequencies (i.e., 5–10 Hz).

In this article, we present a new analytical method to compute the eddy-current loss in thick laminations with a 2-D approach and accounting for the skin effect in the lamination cross section. For this purpose, the eddy-current loss for the studied samples is segregated using a 2-D FE model presented in [7]. Afterward, a time-domain eddy-current loss model is derived based on the analytical solution of 2-D field problem. The FE-based segregated eddy-current loss is then used as a reference to develop the proposed eddy-current loss model in the frequency-domain for sinusoidally varying flux density including a skin effect correction factor. A new phenomenological approach for including the skin effect in the nonlinear region is applied in the modeling. Highly accurate results are obtained with the proposed model compared to the FE reference.

II. Measurements and FE-Based Loss Segregation

Measurements were carried out on toroidal samples cut from typical 3, 6, and 12 mm S275JR grade structural steel laminations used in the rotor pole shoes of large synchronous motors. The toroidal samples are made up of different numbers of laser-cut insulated concentric rings and have the same external geometry. Examples of the used samples are shown in Fig. 1(a). Magnetic measurements were carried out in the range of 0.5–1.5 T magnetization levels, for the quasi-static and sinusoidal excitation cases at 5 and 10 Hz, and the iron loss density was calculated from the measured quantities. The measurement system is described in [7] in detail.

Manuscript received 8 February 2022; revised 14 March 2022; accepted 24 March 2022. Date of publication 28 March 2022; date of current version 26 August 2022. Corresponding author: I. T. Gürbüz (e-mail: ismet.t.gurbuz@aalto.fi).

Color versions of one or more figures in this article are available at https://doi.org/10.1109/TMAG.2022.3162955.

Digital Object Identifier 10.1109/TMAG.2022.3162955

This work is licensed under a Creative Commons Attribution 4.0 License. For more information, see https://creativecommons.org/licenses/by/4.0/

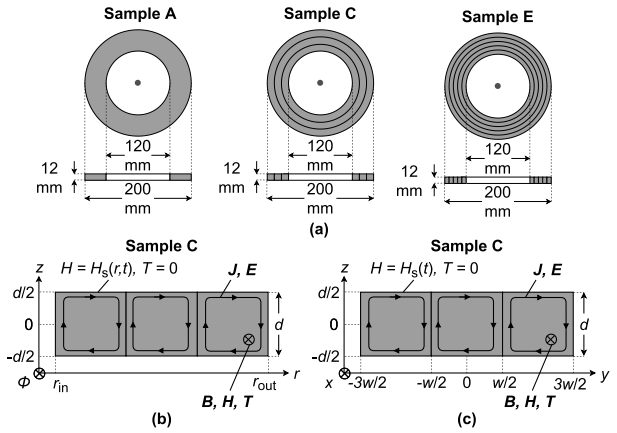

Fig. 1. (a) Top view and cross section of samples A, C, and E constructed from 12 mm laminations. Samples A–E are assembled from 1 to 5 concentric rings, which are 40, 20, 13.3, 10, and 8 mm wide, respectively. In a similar manner, other sets are assembled by using four insulated layers of 3 mm laminations, and two insulated layers of 6 mm laminations to form the same external dimensions. Problem setting for the lamination cross section of sample C constructed with 12 mm lamination is given in (b) cylindrical and (c) Cartesian coordinate systems.

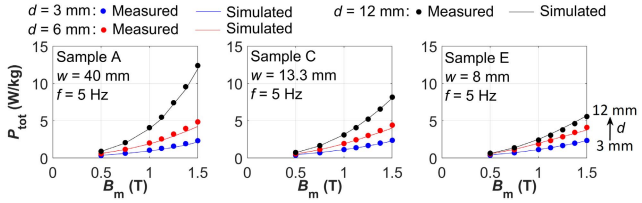

Fig. 2. Comparison of measured (circles) and simulated (solid lines) total losses p_{tot} with 2-D axisymmetric FE model at 5 Hz for samples A, C, and E. Different colors illustrate different d. For each sample, p_{tot} increases as d increases. For a fixed d, p_{tot} reduces as w reduces (from samples A to E).

The 2-D axisymmetric FE model presented in [7] is used for identification of material parameters and simulation of the total losses based on the measurement results. The model considers the cross section of the lamination in the rz plane, along which the current density $\boldsymbol{J}$ is aligned. The magnetic flux density $\boldsymbol{B}$, the magnetic field strength $\boldsymbol{H}$, and the electric vector potential $\boldsymbol{T}$ vectors are considered in the ϕ-direction [see Fig. 1(b)]. At the outer surface of the problem $\boldsymbol{H} = H_{\text{s}}(r, t)$. The defined problem is solved numerically in a MATLAB-based in-house code by using $\boldsymbol{T\Omega}$ formulation with a constitutive material law based on scalar Jiles–Atherton (JA) hysteresis model [11]. The details of the formulation of the model and the solution procedure is presented in [7]. The total losses p_{tot} are simulated with a mean relative error of 4.1% against the measurements for the average magnetic flux density B_{m} levels between 0.5 and 1.5 T as shown in Fig. 2.

The results from the axisymmetric case form a background for developing the model in the Cartesian coordinate system. This development is considered to be necessary for the coupling of the developed model with the 2-D field solution generally used in the analysis of electrical machines. For this purpose, we defined a new problem setting for the lamination cross section in Cartesian coordinate system [see Fig. 1(c)]. The lamination cross section is considered to be in the yz plane. $\boldsymbol{H}(y, z, t) = H(y, z, t)\boldsymbol{u}_x$, $\boldsymbol{B}(y, z, t) = B(y, z, t)\boldsymbol{u}_x$, and $\boldsymbol{T}(y, z, t) = T(y, z, t)\boldsymbol{u}_x$ depend on the position y along the width w and z along the thickness d, and they are

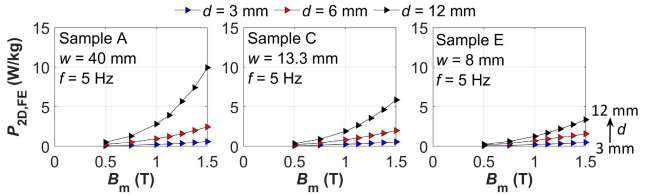

Fig. 3. Simulated eddy-current loss $p_{\text{2D,FE}}$ in 2-D Cartesian FE model at 5 Hz for samples A, C, and E. Different colors illustrate different d. For each sample, $p_{\text{2D,FE}}$ increases as d increases. For a fixed d, p_{tot} reduces as w reduces (from samples A to E). The results are similar for $f = 10$ Hz.

considered to be constant along the x-direction. $\boldsymbol{J}(y, z, t) = J_y(y, z, t)\boldsymbol{u}_y + J_z(y, z, t)\boldsymbol{u}_z$ is considered to be perpendicular to $\boldsymbol{H}$, $\boldsymbol{B}$ and $\boldsymbol{T}$. With the described problem setting in Fig. 1(c), the eddy-current loss coupled with hysteresis loss are simulated for all samples, and then segregated into hysteresis and eddy-current losses. The segregated eddy-current loss from FE solution $p_{\text{2D,FE}}$ is given in Fig. 3.

III. Analytical Model

The results in Fig. 3 indicate that, qualitatively, eddy-current loss increases significantly for all samples as d increases. Also, the eddy-current loss for each set decreases as w decreases as also observed in [7] due to the return path of the eddy currents. However, the quantitative changes are different, which shows that eddy-current loss changes as a function of both d and w. In this section, we present an analytical model for eddy-current loss based on this dependency by taking the FE-based loss segregation as a reference. It should be noted that for the remainder of the article, the term p_{e} will be used as a general term for the eddy-current loss, and the term $p_{\text{2D,FE}}$ will be used for the eddy-current loss obtained from the FE reference.

A. Two-Dimensional Eddy-Current Loss Model

For the problem defined in Fig. 1(c), considering the constitutive law $\mathbf{J} = \sigma \boldsymbol{E}$, where σ is the electrical conductivity and $\boldsymbol{E}$ is the electric field strength, and combining it with Ampere's and Faraday's laws, the 2-D problem can be expressed as

$$\nabla^2 H(y, z, t) = \sigma \frac{\partial B(y, z, t)}{\partial t}. \tag{1}$$

We assume a quadratic spatial dependency for $H(y, z, t)$ as

$$H(y, z, t) = H_{\text{s}}(t) + a(t)\left(y - (w/2)^2\right)\left(z - (d/2)^2\right) \tag{2}$$

where $H_{\text{s}}(t)$ is the magnetic field strength at the surface of the lamination. Parameter $a(t) = (-3/(d^2 + w^2))\partial_t B_0(t)$ is solved by requiring the average of $\sigma^{-1}\nabla^2 H(y, z, t)$ over $[-(w/2)(w/2)] \times [-(d/2)(d/2)]$ to be equal to the rate-of-change of the desired average flux density $B_0(t)$. The material law $H_{\text{Fe}}(B)$ is then expressed weakly by requiring the average of $H(y, z, t)$ to be equal to $H_{\text{Fe}}(B_0)$. This finally gives

$$H_{\text{s}}(t) = H_{\text{Fe}}(B_0(t)) + \frac{\sigma d^2 w^2}{12(d^2 + w^2)} \frac{\partial B_0(t)}{\partial t} \tag{3}$$

which resembles the 1-D *low-frequency approach* for eddy-current loss [10] and reduces to it when $w \gg d$. Average gravimetric loss density p_{av} over one period T of a closed cycle can be computed using (3) such that

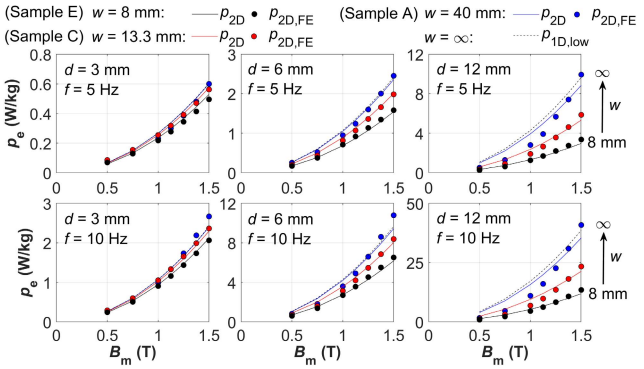

Fig. 4. Comparison of 1-D and 2-D *low-frequency approaches* $p_{1D,low}$ (dashed lines) and $p_{2D,low}$ (solid lines) with the 2-D FE results $p_{2D,FE}$ (circles) for 5 and 10 Hz. Each graph shows the eddy-current loss for samples A, C, and E with same d. Different colors in each graph illustrate different w. $p_{2D,low}$ and $p_{1D,low}$ are similar when $w \to \infty$. When $w \approx d$, estimation of $p_{1D,low}$ is poor, while $p_{2D,low}$ estimates the pattern successfully.

$p_{av} = (\rho T)^{-1} \int_0^T H_s(t)\partial_t B_0(t)dt$, where ρ is the mass density. When $B_0(t)$ is sinusoidal such that $B_0(t) = B_m \sin(2\pi f t)$, the integration of the dynamic term of $H_s(t)$ reduces to

$$p_{2D,low}(f, B_m) = \frac{\sigma \pi^2}{6\rho} \frac{d^2 w^2}{d^2 + w^2} f^2 {B_m}^2. \tag{4}$$

Initially, the eddy-current loss for 5 and 10 Hz frequencies are approximated with $p_{2D,low}$ in (4) and compared with the FE reference $p_{2D,FE}$ and the 1-D *low-frequency approximation* $p_{1D,low}(f, B_m) = (\sigma \pi^2 d^2/6\rho) f^2 B_m^2$ (see Fig. 4). Fig. 4 shows that $p_{2D,low}$ successfully models the pattern of the eddy-current loss as a function of w, which cannot be achieved with the 1-D model. Furthermore, the eddy-current loss for the $d = 3$ mm sheet at both frequencies and the $d = 6$ mm sheet at 5 Hz is estimated fairly well. However, the estimation becomes poorer for the other cases due to skin effect, which increases as d and f increases. While the losses in the linear region are overestimated, the losses in the nonlinear region are underestimated when the skin effect is significant.

B. Correction for Skin Effect

In the linear case with a permeability μ, the 2-D problem in (1) can be solved analytically by separation of variables [12]. This gives a magnetic field distribution of $H(y, z) = H_s h(y, z)$, where $h(y, z)$ is

$$h(y,z) = \frac{\cosh\left(\frac{1+j}{\sqrt{2}}\frac{y}{\delta}\right)\cosh\left(\frac{1+j}{\sqrt{2}}\frac{z}{\delta}\right)}{\cosh\left(\frac{1+j}{\sqrt{2}}\frac{w}{2\delta}\right)\cosh\left(\frac{1+j}{\sqrt{2}}\frac{d}{2\delta}\right)} + \sum_m \frac{\frac{4}{m\pi}\sin\left(\frac{m\pi}{2}\right)}{1 - j\left(\frac{m\pi\delta}{w}\right)^2}\cos\left(\frac{m\pi y}{w}\right)\frac{\cosh\left(\sqrt{2j + \left(\frac{m\pi\delta}{w}\right)^2}\frac{z}{\delta}\right)}{\cosh\left(\sqrt{2j + \left(\frac{m\pi\delta}{w}\right)^2}\frac{d}{2\delta}\right)} + \sum_n \frac{\frac{4}{n\pi}\sin\left(\frac{n\pi}{2}\right)}{1 - j\left(\frac{n\pi\delta}{d}\right)^2}\cos\left(\frac{n\pi z}{d}\right)\frac{\cosh\left(\sqrt{2j + \left(\frac{n\pi\delta}{d}\right)^2}\frac{y}{\delta}\right)}{\cosh\left(\sqrt{2j + \left(\frac{n\pi\delta}{d}\right)^2}\frac{w}{2\delta}\right)}. \tag{5}$$

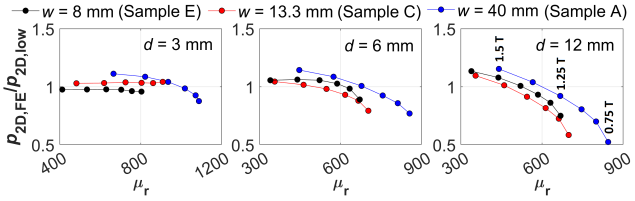

Fig. 5. $p_{2D,FE}/p_{2D,low}$ ratio as a function of relative permeability μ_r for 0.75 T < B_m < 1.5 T at 10 Hz. In each graph, the ratios for samples A, C, and E are demonstrated for each case of d separately. Note the exponential relationship from the presented graphs.

Here, m and n are odd harmonics and $\delta = 1/\sqrt{\pi f \mu \sigma}$ is the skin depth. Due to linearity, the $h(y, z)$ distribution can be directly scaled to obtain any desired value of B_m, which allows us to calculate the eddy-current loss $\tilde{p}_{2D}$ analytically as

$$\tilde{p}_{2D}(f, B_m) = \mathrm{Re}\{j(2\pi f) B_m H_s^*\}$$

with

$$H_s = \left(\frac{\mu}{wd}\int_{-d/2}^{d/2}\int_{-w/2}^{w/2} h(y,z)dydz\right)^{-1} B_m. \tag{6}$$

From (5) and (6), we can estimate the low-frequency limit of the eddy-current loss by assuming that without skin effect, the loss obeys a quadratic dependency on the frequency similar to (4)

$$\tilde{p}_{2D,low}(f, B_m) = f^2 \lim_{f \to 0} (\tilde{p}_{2D}(f, B_m)/f^2) \tag{7}$$

where $\tilde{p}_{2D,low}$ is the eddy-current loss at low frequency in linear region. It turns out that the low-frequency limit (7) does not exactly match with (4). However, we can use (6) and (7) to define a skin-effect factor describing the ratio between the exact loss and the low-frequency loss in the linear region as

$$F_{lin}(f) = \tilde{p}_{2D}(f, B_m)/\tilde{p}_{2D,low}(f, B_m) \tag{8}$$

which is independent of B_m. Although it is difficult to obtain a closed-form expression for (8) due to the infinite sums required in $h(y, z)$, we can still easily evaluate (8) by summing up the terms until a desired accuracy is obtained. This factor can then be used to correct the loss in the linear region.

To account for the transition from linear to nonlinear regions after a given threshold flux-density amplitude B_t, we investigated the relationship between $p_{2D,FE}$ and $p_{2D,low}$ in the range of 0.75–1.5 T magnetization levels. In Fig. 5 the $p_{2D,FE}/p_{2D,low}$ ratio is shown as a function of the relative permeability μ_r identified from the FE model for each sample.

Fig. 5 shows that the behavior of the $p_{2D,FE}/p_{2D,low}$ ratio as a function of μ_r for each case can be approximated by an exponential relationship in the nonlinear region, for which we considered the threshold B_t to be between 0.75–1 T. The characteristics of the exponential curves for each d and w combination are different as the significance of the skin effect varies depending on d and w. For instance, for $d = 3$ mm and $w = 8$ mm, the $p_{2D,FE}/p_{2D,low}$ ratio is close to 1 for each flux density value; whereas, for $d = 12$ mm and $w = 40$ mm, the ratio changes between 0.52 and 1.15 when the flux density changes from 0.75 to 1.5 T. Furthermore, the pattern of the curves indicates that the saturation is reached

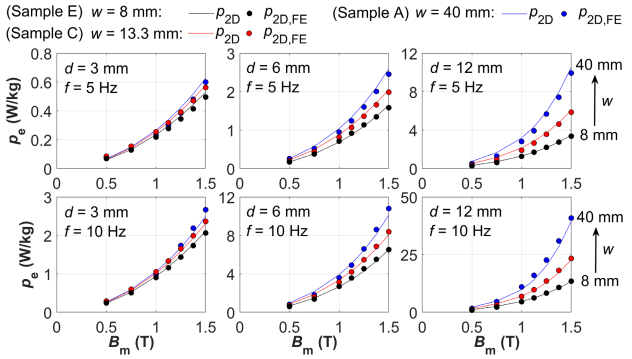

Fig. 6. Comparison of the proposed calculation p_{2D} (solid lines) with the 2-D FE results $p_{2D,FE}$ (circles). Each graph shows the eddy-current loss for samples A, C, and E with same d. Different colors in each graph illustrate different w. With the included skin-effect correction factor $F(f, B_m)$, (11) estimates the eddy-current loss for all cases successfully.

at low permeability/high flux density values. In light of these analyses, we define an empirical correction factor $F_{non}(f, B_m)$ for the nonlinear region $B_m \geq B_t$ as

$$F_{non}(f, B_m) = k + 1 - e^{\tau(f)(\mu(B_m)-\mu_0)}$$

with

$$\tau(f) = \ln(k + 1 - F_{lin}(f))/(\mu(B_t) - \mu_0). \tag{9}$$

Here, k is the only fitting coefficient, and τ is the coefficient which ensures the continuity at $B_m = B_t$ so that $F_{lin} = F_{non}$. $F_{non}(f, B_m)$ extrapolates to k when $\mu = \mu_0$. In its final form, the skin-effect factor $F(f, B_m)$ can be expressed as

$$F(f, B_m) = \begin{cases} F_{lin}(f), & B_m \leq B_t \text{ (linear region)} \\ F_{non}(f, B_m), & B_m \geq B_t \text{ (nonlinear region)} \end{cases} \tag{10}$$

which enables the calculation of eddy-current loss in 2-D with skin-effect correction such that

$$p_{2D}(f, B_m) = p_{2D,low}(f, B_m) F(f, B_m). \tag{11}$$

We assumed that $B_t = 0.75$ T and performed least-squares fitting for each d and w combination separately, as their identified B–H curves in FE model vary. Therefore, τ parameters are calculated for each permeability, and k is fit for each d and w combination. Estimated eddy-current loss with the fit coefficients are illustrated in Fig. 6.

Fig. 6 shows that the eddy-current loss for each case is obtained with a high accuracy. The mean relative error for all the cases is 8.1%. For the nonlinear part, $B_m > 0.75$ T, the mean relative error is 5.1%, which shows the applicability of the derived mathematical expression in (9). The details of the relative error in the nonlinear region for all combinations are given in Table I. The estimated F_{non} and $p_{2D,FE}/p_{2D,low}$ ratio for 12 mm laminations are compared in Fig. 7.

The coefficients of the proposed correction factor F_{non} are kept constant for different frequencies for simplicity. Therefore, the model estimates the exponential relationship in average. The errors presented in Table I prove the accuracy of the proposed method, which successfully estimates the eddy-current loss for several cases.

TABLE I
RELATIVE ERROR IN THE NONLINEAR REGION

f	d	w 8 mm	10 mm	13.3 mm	20 mm	40 mm
5 Hz	3 mm	7.2%	9.3%	1.7%	9.0%	**11.5%**
	6 mm	3.1%	1.3%	4.5%	6.5%	6.9%
	12 mm	1.2%	2.3%	6.6%	7.8%	8.8%
10 Hz	3 mm	2.3%	3.0%	3.5%	2.3%	4.4%
	6 mm	3.7%	2.5%	3.5%	7.4%	4.9%
	12 mm	2.3%	2.4%	3.5%	5.2%	10.6%

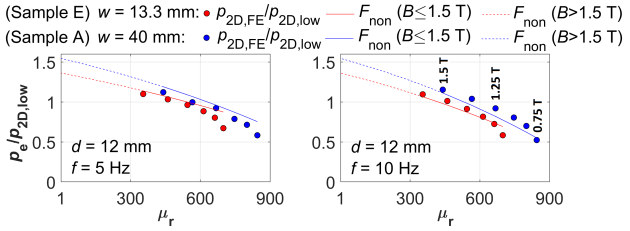

Fig. 7. Comparison of the $p_{2D,FE}/p_{2D,low}$ ratio (circles) and estimation of the model F_{non} (solid lines) for $d = 12$ mm with fit parameter $k = 1.54$ for $w = 40$ mm and $k = 1.36$ for $w = 13.3$ mm cases, respectively. The dashed lines show the extrapolation of F_{non} for μ_r when $B_m > 1.5$ T.

IV. CONCLUSION

In this article, we present two main contributions. First, we propose a simple time-domain eddy-current model for thick laminations. Then, we obtain a simple frequency-domain eddy-current model for sinusoidally varying flux density and modify it with a skin-effect correction accounting for the material's nonlinearity. Incorporation of the models to the machine simulation should be investigated in further studies.

REFERENCES

[1] O. Bottauscio and M. Chiampi, "Analysis of laminated cores through a directly coupled 2-D/1-D electromagnetic field formulation," *IEEE Trans. Magn.*, vol. 38, no. 5, pp. 2358–2360, Sep. 2002.
[2] E. Dlala, A. Belahcen, and A. Arkkio, "Efficient magnetodynamic lamination model for two-dimensional field simulation of rotating electrical machines," *J. Magn. Magn. Mater.*, vol. 320, no. 20, pp. e1006–e1010, Oct. 2008.
[3] J. Gyselinck, R. V. Sabariego, and P. Dular, "A nonlinear time-domain homogenization technique for laminated iron cores in three-dimensional finite-element models," *IEEE Trans. Magn.*, vol. 42, no. 4, pp. 763–766, Apr. 2006.
[4] O. Bottauscio, M. Chiampi, and D. Chiarabaglio, "Advanced model of laminated magnetic cores for two-dimensional field analysis," *IEEE Trans. Magn.*, vol. 36, no. 3, pp. 561–573, May 2000.
[5] S. Elfgen, P. Rasilo, and K. Hameyer, "Hysteresis and eddy-current losses in electrical steel utilising edge degradation due to cutting effects," *Int. J. Numer. Model., Electron. Netw., Devices Fields*, vol. 33, no. 5, p. e2781, 2020.
[6] P. Rasilo, W. Martinez, K. Fujisaki, J. Kyyrä, and A. Ruderman, "Simulink model for PWM-supplied laminated magnetic cores including hysteresis, eddy-current, and excess losses," *IEEE Trans. Power Electron.*, vol. 34, no. 2, pp. 1683–1695, Feb. 2019.
[7] I. T. Gurbuz *et al.*, "Finite-element modeling and characterization of iron losses in 12 mm thick steel laminations including the effect of cutting," *IEEE Access*, vol. 9, pp. 115710–115718, 2021.
[8] E. Dlala, "A simplified iron loss model for laminated magnetic cores," *IEEE Trans. Magn.*, vol. 44, no. 11, pp. 3169–3172, Nov. 2008.
[9] S. E. Zirka, Y. I. Moroz, P. Marketos, and A. J. Moses, "Loss separation in nonoriented electrical steels," *IEEE Trans. Magn.*, vol. 46, no. 2, pp. 286–289, Sep. 2010.
[10] G. Bertotti, *Hysteresis in Magnetism*. San Diego, CA, USA: Academic, 1998.
[11] D. C. Jiles, J. B. Thoelke, and M. K. Devine, "Numerical determination of hysteresis parameters for the modeling of magnetic properties using the theory of ferromagnetic hysteresis," *IEEE Trans. Magn.*, vol. 28, no. 1, pp. 27–35, Jan. 1992.
[12] E. Voipio, *Kenttäteoria*. Helsinki, Finland: Otakustantamo, 1987.